

# Interference between extrinsic and intrinsic losses in x-ray absorption fine structure

L. Campbell,<sup>1</sup> L. Hedin,<sup>2</sup> J. J. Rehr,<sup>1</sup> and W. Bardyszewski<sup>3</sup>

<sup>1</sup>*Department of Physics, University of Washington, Seattle, Washington 98195-1560*

<sup>2</sup>*Department of Physics, Lund University, Lund, S22362 Sweden  
and MPI-FKF, Stuttgart, D70569 Germany*

<sup>3</sup>*Department of Physics, Institute of Theoretical Physics, 00-681 Warsaw, Poland*

(Received 28 March 2001; revised manuscript received 16 October 2001; published 22 January 2002)

The interference between extrinsic and intrinsic losses in x-ray absorption fine structure (XAFS) is treated within a Green's-function formalism, without explicit reference to final states. The approach makes use of a quasiboson representation of excitations and perturbation theory in the interaction potential between electrons and quasibosons. These losses lead to an asymmetric broadening of the main quasiparticle peak plus an energy-dependent satellite in the spectral function. The x-ray absorption spectra (XAS) is then given by a convolution of an effective spectral function over a one-electron cross section. It is shown that extrinsic and intrinsic losses tend to cancel near excitation thresholds, and correspondingly, the strength in the main peak increases. At high energies, the theory crosses over to the sudden approximation. These results thus explain the observed weakness of multielectron excitations in XAS. The approach is applied to estimate the many-body corrections to XAFS, beyond the usual mean-free path, using a phasor summation over the spectral function. The asymmetry of the spectral function gives rise to an additional many-body phase shift in the XAFS formula.

DOI: 10.1103/PhysRevB.65.064107

PACS number(s): 78.70.Dm, 71.10.-w

## I. INTRODUCTION

The treatment of inelastic losses in x-ray absorption fine structure (XAFS) has long been of interest.<sup>1-3</sup> Two types of losses are identified. *Extrinsic* losses occur during the propagation of the photoelectron, and are caused by the creation of excitations such as plasmons, electron-hole pairs, etc. *Intrinsic* losses refer to the creation of excitations by the sudden appearance of the core hole. The intrinsic losses are often called shake-up and shake-off excitations but are of the same type as the extrinsic, i.e., plasmons, multielectron excitations, etc. Typically these excitations are observed only weakly in x-ray absorption spectra (XAS). The extrinsic losses cause a decrease in intensity in the no loss or primary channel, which is usually treated phenomenologically in terms of a mean-free path  $\lambda$ . Owing to the difficulty of quantitative calculations, these additional losses have usually been neglected or represented as a constant-amplitude factor, on the understanding that they only give some smooth background.

The question of possible *interference* between extrinsic and intrinsic losses has long been unsettled. For photoemission spectroscopy, it has been shown<sup>4,5</sup> that this interference is particularly important near excitation thresholds, where the losses strongly cancel. This cancellation results from the opposite signs of the coupling between the photoelectron and the core hole to excited states of the valence electrons. In particular, for plasmon creation at threshold, only the long-wavelength plasmons appear, which, due to momentum conservation, makes the recoil of the electron in the extrinsic losses small. The intrinsic losses are caused by coupling to the core hole, which cannot recoil. As a result the extrinsic and intrinsic couplings become equal at threshold. The situation in XAFS is less clear. Fujikawa has discussed this cancellation using an explicit calculation of matrix elements and approximate closure relations.<sup>6</sup> However, his discussion is

limited to the vicinity of threshold, while we find that the cancellation effects extend over a wide energy region.

In this paper, we present a formal analysis of the loss problem, which is an extension of work by Hedin and Bardyszewski,<sup>2,3,5</sup> together with numerical calculations to illustrate the theory. The results here are formulated in terms of an effective one-particle propagator that includes both inelastic losses and interference effects. This propagator contains an asymmetric quasiparticle peak plus a broad energy-dependent satellite structure. Our approach is essentially a generalization of the "GW approximation" (see below) which, in addition to extrinsic losses, treats *intrinsic* losses and *interference* terms. The formalism also partly accounts for edge-singularity effects and contains corrections to the final state rule. Although the cumulant expansion was successfully used to describe *intrinsic* losses in valence-electron photoemission,<sup>7</sup> we have found it more difficult to apply for x-ray absorption spectra. For photoemission (PES) the propagator for a hole and the spectral function  $A^h(\omega) = A(\omega)\theta(E_F - \omega)$  are needed, while in XAS we need the propagator for a particle and the spectral function  $A^p(\omega) = A(\omega)\theta(\omega - E_F)$ . The GW approximation for  $A(\omega)$  was discussed in Ref. 8 (pp. 87, 92). The satellite of the hole spectral function is very strong and sharp at the bottom of the band, but decreases in intensity and broadens as one approaches the Fermi energy  $E_F$ .<sup>8,9</sup> At  $E_F$ , the satellite for the particle spectrum is similar to that for the hole spectrum, and it rapidly becomes weaker and broader with increasing energy above  $E_F$ . The GW approximation places the satellite at about  $1.5\omega_p$ , rather than at  $\omega_p$  away from the quasiparticle peak, as is predicted by the cumulant approximation, and born out by PES experiments.<sup>7</sup> However, above the Fermi level the difference between the GW and cumulant approximations is less pronounced.

Our formulation clarifies the nature of inelastic losses in XAS and also yields semiquantitative estimates of their effects, based on the electron-gas approximation. In particular, the theory yields an estimate for the reduction in the XAFS

amplitude due to inelastic losses in terms of a phasor summation over the spectral function. This results in an energy-dependent reduction factor  $|S_0^2(\omega)|$  to the usual XAFS formula, as well as an additional many-body phase shift. Near the excitation threshold, we find that there is appreciable cancellation of strong extrinsic and intrinsic losses by the interference terms. Correspondingly, the strength of the primary channel, i.e., the main quasiparticle peak, increases near threshold. Thus the theory also explains the surprising weakness of multielectron excitations in the observed XAS.<sup>10</sup> At sufficiently high energies both the extrinsic and the interference contributions become negligible, and the theory crosses over to the sudden-approximation limit, where only intrinsic losses remain. Our theory is illustrated for the case of Cu metal. This system provides a good test case for our theory since errors in the conventional multiple scattering (MS) expansion and potentials are minimal and accurate experimental data are available.<sup>11</sup>

## II. THEORY

### A. Basic expressions

The x-ray absorption coefficient  $\mu(\omega)$  can be expressed formally in terms of the many-electron Green's function  $G(E) = 1/(E - H + i\gamma)$  as

$$\mu(\omega) = -\frac{1}{\pi} \text{Im} \left\langle \Psi_0 \left| \Delta^\dagger \frac{1}{E_0 + \omega - H + i\gamma} \Delta \right| \Psi_0 \right\rangle, \quad (1)$$

where  $|\Psi_0\rangle$  is the  $N$ -particle ground state of the total system (valence electrons and ion cores),  $H$  the Hamiltonian that fully includes electron-electron interactions,  $E_0$  the ground-state energy (we consider for simplicity only the case when the temperature is zero), and  $\omega$  the photon energy. We use atomic units  $m = |e| = \hbar = 1$ , where lengths are in Bohr radii (0.529 Å) and energies in Hartrees (27.2 eV). Further

$$\Delta = \sum_k \langle k | d | b \rangle c_k^\dagger b + h.c., \quad (2)$$

is the dipole operator coupling the photon to the electronic system, and  $\gamma$  the inverse core-hole lifetime. We have assumed that a specific core level  $|b\rangle$  on a specific atom is involved.

The standard way to proceed from Eq. (1) is to insert a complete set of interacting states  $|\Psi_n\rangle$ , which recovers the golden-rule expression when we take  $\gamma$  as infinitesimal; a finite  $\gamma$  just gives a Lorentzian broadening, i.e.,

$$\mu(\omega) = \sum_n |\langle \Psi_n | \Delta | \Psi_0 \rangle|^2 \delta(E_0 + \omega - E_n). \quad (3)$$

This expression contains explicit final states  $|\Psi_n\rangle$  in which the excited electron (the photoelectron) is correlated with the valence electrons. Such states are very difficult to handle, so we instead take a different route that leads to an expression where no explicit final states are involved but instead, an expansion in one-electron Green's functions, as in conventional XAS theory. Our formulation, however, contains

shake-up effects and extrinsic inelastic losses as well as interference terms, and not just the damping in the elastic channel.

Some of the formal results derived here were presented previously in short conference reports.<sup>2,3</sup> In this paper, we have concentrated on the shake-up effects of the core-hole potential and on the extrinsic losses of the ejected electron. To have a clean picture, we have regarded the core electron as structureless. Thus we have not considered interesting problems like core-hole degeneracies and  $L_{II}/L_{III}$  edges. Such problems are, in principle, complicated Kondo-type problems. If we, however, limit the treatment to have an ion embedded in a solid-state environment, and only consider the multiplet effects for the embedded ion,<sup>12</sup> we think our treatment could straightforwardly be extended to this situation.

We take for  $H$  the standard ‘‘deep-level’’ Hamiltonian discussed, e.g., by Langreth<sup>13</sup> (cf. Ref. 14, p. 645),

$$H = H_v + \varepsilon_c b^\dagger b + V b b^\dagger. \quad (4)$$

Here  $H_v$  describes the electrons outside the ion cores, i.e., the valence electrons and the photoelectron, and  $V$  the interactions between the outer electrons and the core hole. This approximation neglects virtual excitations of the core electrons, but takes correlations among the outer electrons and the potential  $V$  from the core hole fully into account. Neglecting core-valence exchange we have explicitly,

$$V = - \sum_i w(\mathbf{r}_i), \quad w(\mathbf{r}) = \int v(\mathbf{r} - \mathbf{r}') \rho_b(\mathbf{r}') d\mathbf{r}', \quad (5)$$

where  $v(\mathbf{r})$  is the Coulomb potential, and  $\rho_b(\mathbf{r})$  the charge density of the core electron state ‘‘ $b$ .’’ The ground state of  $H|\Psi_0\rangle$ , is thus a product,

$$|\Psi_0\rangle = |\Phi_0\rangle |b\rangle, \quad (6)$$

where  $|\Phi_0\rangle$  is the correlated wave function for  $N_v$  outer electrons and  $|b\rangle$  is the core electron wave function,

$$H_v |\Phi_0\rangle = E_0^0 |\Phi_0\rangle, \quad H |\Psi_0\rangle = E_0 |\Psi_0\rangle, \quad E_0 = E_0^0 + \varepsilon_c.$$

The passive core electrons are not written out explicitly. The core electrons are easily eliminated, and Eqs. (1), (2), and (6) give

$$\mu(\omega) = -\frac{1}{\pi} \text{Im} \sum_{k_1, k_2} \langle b | d^\dagger | k_1 \rangle \langle k_2 | d | b \rangle \times \left\langle \Phi_0 \left| c_{k_1} \frac{1}{E_0 + \omega - H'_v + i\gamma} c_{k_2}^\dagger \right| \Phi_0 \right\rangle, \quad (7)$$

where

$$H'_v = H_v + V.$$

Here and elsewhere in this paper, we will use a prime to denote quantities calculated in the presence of a core hole. The x-ray absorption is now formally given by a one-electron expression

$$\mu(\omega) = -\frac{1}{\pi} \text{Im} \sum_{k_1 k_2} \langle b | d^\dagger | k_1 \rangle \langle k_1 | g_{\text{eff}}(\omega + E_c) | k_2 \rangle \langle k_2 | d | b \rangle, \quad (8)$$

where  $g_{\text{eff}}(\omega)$  is an “effective” one-electron Green’s function

$$\langle k_1 | g_{\text{eff}}(\omega) | k_2 \rangle = \left\langle \Phi_0 \left| c_{k_1} \frac{1}{\omega - (H'_v - E'_0) + i\gamma} c_{k_2}^\dagger \right| \Phi_0 \right\rangle. \quad (9)$$

The quantity  $E'_0$  is the ground-state energy of  $H'_v$  for  $N_v$  electrons, and  $E_c = \varepsilon_c + E'_0 - E_0$  is the renormalized core-electron energy. This Green’s function is not of standard form since  $|\Phi_0\rangle$  is an eigenfunction of  $H_v$  and we have  $H'_v$  in the denominator.

The theory developed so far is quite general, and can even account for losses, threshold singularity effects, and deviations from the “final state rule,” i.e., the prescription that the XAS is given by a one-electron expression with dipole-matrix elements between the initial-core and final-state wave functions calculated in the presence of the core hole. The function  $\mu(\omega)$  is always positive, and  $g_{\text{eff}}$  can be written in terms of a Hermitian spectral function. An approximation for the “transient” Green’s function in Eq. (9) to describe the edge shape was given in Ref. 14, p. 674. However, here we want to describe loss processes, and thus we have to develop different approximations. These approximations, as discussed below, can be summed up in the quasiboson representation described in Sec. II C.

To get a qualitative feeling for the properties of the transient Green’s function, we first discuss them in the Hartree-Fock approximation. The ground state of  $H_v$ ,  $|\Phi_0\rangle$  then is a Slater determinant, and the intermediate states in Eq. (9) are Slater determinants built from orbitals that are self-consistent solutions of a Schrödinger equation with the core-hole Hamiltonian  $H'_v = H_v + V$ . We are free to choose any complete set to represent the states  $k$  in the optical transition operator  $\Delta = \sum_k \langle k | d | b \rangle c_k^\dagger b$ . Here, we take the states that belong to  $H_v$ , which have the convenient property that  $c_k^\dagger |\Phi_0\rangle = 0$  for  $k < k_F$ . In  $H'_v$  we single out one term  $h'$  with orbitals that describe the photoelectron, and one  $H'_{v0}$  with orbitals for the rest of the system,

$$H'_v = h' + H'_{v0}. \quad (10)$$

These two terms both have interactions with the core hole,  $V_{pc}$  and  $V_{vc}$ , respectively, which are screened versions of  $V$  in Eq. (5), since we consider a self-consistent Hartree-Fock (HF) solution for the core-hole Hamiltonian. In terms of the old Hamiltonian  $H_v = h + H_{v0}$ ,

$$h' = h + V_{pc}, \quad H'_{v0} = H_{v0} + V_{vc}. \quad (11)$$

With the  $h'$  orbitals separated from the  $H'_{v0}$  orbitals, only the one-electron operator  $h'$  can couple  $c_{k_2}^\dagger$  to  $c_{k_1}$  in Eq. (9). In such a case we can use a product space,  $c_k^\dagger |\Phi_0\rangle = |\Phi_0\rangle |k\rangle$ , which then gives for the many-body XAS,

$$\mu(\omega) = -\frac{1}{\pi} \text{Im} \langle b | d^\dagger P g_{\text{eff}}(\omega + E_c) P d | b \rangle, \quad (12)$$

where

$$g_{\text{eff}}(\omega) = \left\langle \Phi_0 \left| \frac{1}{\omega - (H'_v - E'_0) + i\gamma} \right| \Phi_0 \right\rangle, \quad (13)$$

and the projection operator onto unoccupied one-particle states of the initial state (without a core hole) is

$$P = \sum_{k > k_F} |k\rangle \langle k|. \quad (14)$$

The separation of  $H'_v$  into  $h'$  and  $H'_{v0}$  is clearly an approximation. However, it makes physical sense and has been used previously, e.g., for photoemission problems.<sup>17</sup> In this expression the coupling between the photoelectron and the valence electrons is not present, since it is a correlation effect beyond the HF approximation. This defect is of less importance for a localized system, where HF theory is often quite useful.

Let us now turn to the correlated case. A correlated  $|\Phi_0\rangle$  can, in principle, be calculated from configuration-interaction theory. Then  $|\Phi_0\rangle$  is a sum of Slater determinants having differing numbers of electron-hole excitations (virtual excitations). The Slater determinants with virtual states close to the Fermi level have the largest coefficients in this expansion. For photoelectron states  $k$  away from this virtual cloud it is a good approximation to use a product space. For definiteness we will use

$$c_k^\dagger |\Phi_0\rangle \approx \begin{cases} |\Phi_0\rangle |k\rangle, & k > k_F \\ 0, & k < k_F \end{cases}, \quad (15)$$

being aware that this is a dangerous approximation for  $k \simeq k_F$ . As before we split  $H'_v$  into one part  $h'$  that describes the photoelectron, and one part  $H'_{v0}$  for other excitations of the valence electrons, and we introduce core-hole potentials as in Eq. (11). In addition we now also have the dynamic coupling  $V_{pv}$  between the photoelectron and the valence electrons,

$$V_{pv} = \sum_{k_1 k_2} \sum_{l_1 l_2}^{\text{val}} \langle k_1 l_1 | v | k_2 l_2 \rangle c_{k_1}^\dagger c_{k_2} [c_{l_1}^\dagger c_{l_2} - \langle c_{l_1}^\dagger c_{l_2} \rangle]. \quad (16)$$

The term  $\langle k_1 l_1 | v | k_2 l_2 \rangle$  is an antisymmetrized matrix element of the Coulomb potential  $v(\mathbf{r})$ , and the expectation value  $\langle c_{l_1}^\dagger c_{l_2} \rangle$  is subtracted, since it is already included in the definition of  $h'$ . The state  $|\Phi_0\rangle$  is an eigenfunction of  $H_{v0}$  built from one-electron eigenfunctions without core-hole potential while  $h'$  is built from eigenfunctions  $|k'\rangle$  with a core hole present,

$$h' = \sum_{k' > k_F} \varepsilon_k |k'\rangle \langle k'|. \quad (17)$$

The states  $|k'\rangle$  are scattering states. There is thus a one-to-one correspondence between  $|k'\rangle$  and  $|k\rangle$ , and the energies

are unchanged. Since  $h'$  only has terms bilinear in the photoelectron operators  $c_k$ , and since there is a linear relation between the states  $|k'\rangle$  and  $|k\rangle$ ,  $h'$  will not take us outside the product space  $|\Phi_0\rangle|k\rangle$ .

From Eqs. (7) and (15), we again obtain Eq. (12) for the XAS, but with  $g_{\text{eff}}(\omega)$  in Eq. (8) replaced by

$$g_{\text{eff}}(\omega) = \left\langle \Phi_0 \left| \frac{1}{\omega - (H'_{v0} - E'_0) - h' - V_{pv} + i\gamma} \right| \Phi_0 \right\rangle. \quad (18)$$

Equations (10), (11), (12), and (18) form the basis for our analysis of x-ray absorption. It is easy to show that Eq. (12) gives a nonnegative absorption cross section  $\mu(\omega)$ , as it should.

### B. Limiting cases

We start our analysis of the theoretical model developed above by discussing the two limiting cases: (1) when there is no extrinsic scattering ( $V_{pv} = 0$ ), and (2) when the core-hole potential is neglected ( $H'_{v0} = H_{v0}$ ).

#### 1. No extrinsic scattering

In this case  $V_{pv} = 0$ , and we can put in a complete set of eigenstates  $|\Phi'_n\rangle$  to  $H'_{v0}$  with eigenvalues  $E'_n$  and obtain (taking  $\gamma$  as an infinitesimal)

$$g_{\text{eff}}(\omega) = \sum_n \frac{|\langle \Phi_0 | \Phi'_n \rangle|^2}{\omega - \omega_n - h' + i\gamma}, \quad (19)$$

where  $\omega_n = E'_n - E'_0$ . Putting in eigenstates  $|k'\rangle$  of  $h'$ , and taking the imaginary part, we then obtain,

$$\begin{aligned} \mu(\omega) &= \sum_{k,n} |\langle \Phi_0 | \Phi'_n \rangle|^2 |\langle k' | P d | b \rangle|^2 \delta(\omega + E_c - \omega_n - \epsilon_k) \\ &= \int_0^{\omega + E_c - E_F} d\omega' A(\omega') \mu^{(1)}(\omega + E_c - \omega'), \end{aligned} \quad (20)$$

where the core-hole spectral function  $A(\omega)$  is

$$A(\omega) = \sum_n |\langle \Phi_0 | \Phi'_n \rangle|^2 \delta(\omega - \omega_n), \quad (21)$$

and the one-electron XAS is

$$\mu^{(1)}(\omega) = \sum_{k' > k_F} |\langle k' | P d | b \rangle|^2 \delta(\omega - \epsilon_k). \quad (22)$$

A similar result was derived and discussed earlier by Rehr *et al.*<sup>1</sup> However, an important difference in our formulation is the presence of the projection operator  $P$  in the dipole-matrix element. It is interesting to note that  $A(\omega)$  contains the core-electron edge singularity  $A(\omega) \approx \omega^{\alpha-1}$ , where  $\alpha$  is the singularity index, and that  $\mu^{(1)}(\omega)$  is also singular at the Fermi level,  $\mu^{(1)}(\omega) \approx (\omega - E_F)^\beta$ . This latter singularity follows from the singular behavior of the overlap integral  $\langle k' | k \rangle$ .<sup>15</sup> We also see from Eq. (22) that the final-state rule is not strictly valid, except well above threshold, where  $P$  can

be replaced by a  $\delta$  function and the matrix element reduces to  $\langle k' | d | b \rangle$ . We know from photoemission<sup>16</sup> that there is little extrinsic scattering at threshold, where this limiting case should be a good representation of our basic approximation given by Eqs. (12) and (18).

#### 2. No core hole

When the core-hole potential is neglected,  $H'_{v0} = H_{v0}$ ,  $h' = h$ , and we have (taking  $\gamma$  as an infinitesimal)

$$g_{\text{eff}}(\omega) = \left\langle \Phi_0 \left| \frac{1}{\omega - (H_{v0} - E_0) - h - V_{pv} + i\gamma} \right| \Phi_0 \right\rangle. \quad (23)$$

Now  $g_{\text{eff}}(\omega)$  is equivalent to a standard Green's function  $g(\omega)$ . The  $k_1 k_2$  representation of  $g(\omega)$  is

$$\begin{aligned} \langle k_1 | g(\omega) | k_2 \rangle &= \langle 0 | \left\langle \Phi_0 \left| c_{k_1} \frac{1}{\omega - (H_{v0} - E_0) - h - V_{pv} + i\gamma} \right. \right. \\ &\quad \left. \left. \times c_{k_2}^\dagger \right| \Phi_0 \right\rangle | 0 \rangle, \end{aligned} \quad (24)$$

where  $|\Phi_0\rangle|0\rangle$  is an eigenfunction of the full Hamiltonian  $H_{v0} + h + V_{pv}$  since  $V_{pv}|0\rangle = 0$ . We can express  $g$  in terms of a spectral function  $A(\omega)$ ,

$$\begin{aligned} \langle k_1 | g(\omega) | k_2 \rangle &= \int_{E_F}^{\infty} \frac{\langle k_1 | A(\omega') | k_2 \rangle d\omega'}{\omega - \omega' + i\gamma} \\ &= \left\langle k_1 \left| \frac{1}{\omega - h - \Sigma(\omega)} \right| k_2 \right\rangle. \end{aligned} \quad (25)$$

This limiting case gives a theory very similar to one-electron theory, but with an additional complex, energy-dependent one-electron potential  $\Sigma(\omega)$ . If we approximate  $\Sigma(\omega)$  by a constant  $-i\Gamma$ , which is equivalent to a Lorentzian line shape for  $A(\omega)$ , we recover the conventional XAFS result, in which extrinsic losses are represented by a mean-free path  $\lambda_k \approx k/\Gamma$  term, i.e., with a factor  $\exp(-R/\lambda_k)$  in each multiple-scattering path of length  $R$ . In general,  $\Sigma(\omega)$  has structure at energies away from the quasiparticle energy, giving rise to satellite effects.

### C. Quasiboson representation

We now turn to the general case, in which all three potentials  $V_{pv}$ ,  $V_{pc}$ , and  $V_{vc}$  that couple the three subsystems—the photoelectron, valence electrons, and core electron—are nonzero. To handle this we introduce a quasiboson model Hamiltonian,

$$H_{v0} = \sum_n \omega_n a_n^\dagger a_n, \quad h' = \sum_{k > k_F} \epsilon_k c_k^\dagger c_k, \quad (26)$$

$$V_{vc} = - \sum_n V_{bb}^n (a_n^\dagger + a_n), \quad (27)$$

$$V_{pv} = \sum_{nk_1k_2} [V_{k_1k_2}^n a_n^\dagger + (V_{k_1k_2}^n)^* a_n] c_{k_1}^\dagger c_{k_2}. \quad (28)$$

This model together with Eqs. (11), (12), and (18) define the set of approximations that we use in this work. The potential  $V_{pc}$  never appears explicitly since  $h|\Phi_0\rangle=0$ , and thus we do not have to worry about the transform between the  $h$  and  $h'$  states.

The quasiboson model has been discussed, e.g., in Refs. 5 and 17. The essence is that the electron-hole-type excitations are represented by bosons  $a_n$  with energies  $\omega_n$ , and the electron-charge fluctuation coupling is represented by a term linear in the boson operators, as in Eq. (28). This is analogous to the usual electron-photon coupling. Equation (27) is a special case of Eq. (28) with  $c_{k_1}^\dagger c_{k_2}$  replaced by  $bb^\dagger$  and a minus sign, because the core-hole potential is attractive. The quantities  $V^n$  are fluctuation potentials corresponding to excited states  $n$ . The  $V^n$  can be obtained, e.g., from an RPA-type dielectric function.<sup>16</sup> With this simple model Hamiltonian we can solve explicitly for the relation between the ground states of  $H_{v0}$  and  $H'_{v0}$ , i.e.,

$$|\Phi_0\rangle = e^{-S} |\Phi'_0\rangle, \quad S = \frac{a}{2} - \sum_n \frac{V_{bb}^n}{\omega_n} \bar{a}_n^\dagger, \quad a = \sum_n \left( \frac{V_{bb}^n}{\omega_n} \right)^2,$$

where  $\bar{a}_n^\dagger$  belongs to  $H'_{v0} = \sum_n \omega_n \bar{a}_n^\dagger \bar{a}_n$ . Expanding to second order in the coupling functions  $V^n$ , we obtain

$$\begin{aligned} g_{\text{eff}}(\omega) &= \left\langle \Phi'_0 \left| e^{-S^\dagger} \frac{1}{\omega - (H'_{v0} - E'_0) - h' - V_{pv} + i\gamma} e^{-S} \right| \Phi'_0 \right\rangle \\ &= e^{-a} \left\{ g(\omega) + \sum_n \left( \frac{V_{bb}^n}{\omega_n} \right)^2 g(\omega - \omega_n) \right. \\ &\quad \left. - 2 \sum_n \frac{V_{bb}^n}{\omega_n} g(\omega - \omega_n) V^n g(\omega) \right\}, \quad (29) \end{aligned}$$

where [cf. Eq. (18)]

$$\begin{aligned} g(\omega) &= \left\langle \Phi'_0 \left| \frac{1}{\omega - (H'_{v0} - E'_0) - h' - V_{pv} + i\gamma} \right| \Phi'_0 \right\rangle \\ &\equiv \frac{1}{\omega - h' - \Sigma(\omega) + i\gamma}, \quad (30) \end{aligned}$$

is the damped Green's function calculated in the presence of a core-hole potential. With the above result for  $g_{\text{eff}}(\omega)$  we have achieved our goal of expressing  $\mu(\omega)$  in Eq. (12) as an expansion in one-particle Green's functions, thus avoiding the calculation of correlated many-body final states. In the next section we take the further step of making a MS expansion of the Green's functions. We note that the limiting expressions in Sec. II B, all come out the same if we had chosen to start with the quasi-boson model.

#### D. Qualitative discussion of second-order expression

While our basic approximation in Eqs. (12) and (18) gives positive absorption  $\mu(\omega)$ , there is no guarantee that the individual terms in an expansion in powers of the coupling func-

tions  $V^n$  should be positive. The coupling strength may be gauged by the value of the dimensionless coefficient  $a$  defined above. For electron-gas models of solids, counting only plasmon modes, its value is typically 0.2–0.4, and hence is quite strong. For values of  $k$  close to the Fermi surface the extrinsic quasiparticle strength  $Z$  is about  $\exp(-a) \approx 0.8$ –0.7. Such values for  $Z$  are typical for most solids. The fact that effects of order  $a$  are *not* generally observed in XAS can be viewed as empirical evidence for strong cancellation effects among the various losses. However, given these large values of  $a$ , it is not surprising to encounter some nonphysical effects in numerical calculations, such as small regions where the spectral function can become negative, which are due to the neglect of terms higher than second order in the theory.

Summarizing our second-order expression, and changing the definition of  $g_{\text{eff}}$  in Eq. (18) by taking out the  $e^{-a}$  factor, we have for the absorption spectrum,

$$\mu(\omega) = -\frac{e^{-a}}{\pi} \text{Im} \langle b | d^\dagger P g_{\text{eff}}(\omega + E_c) P d | b \rangle, \quad (31)$$

where

$$g_{\text{eff}}(\omega) = g_{\text{qp}}(\omega) + g_{\text{extr}}(\omega) + g_{\text{intr}}(\omega) + g_{\text{inter}}(\omega),$$

$$g_{\text{qp}}(\omega) + g_{\text{extr}}(\omega) = g(\omega),$$

$$g_{\text{intr}}(\omega) = \sum_n \left( \frac{V_{bb}^n}{\omega_n} \right)^2 g(\omega - \omega_n),$$

$$g_{\text{inter}}(\omega) = -2 \sum_n \frac{V_{bb}^n}{\omega_n} g(\omega - \omega_n) V^n g(\omega), \quad (32)$$

account, respectively, for the quasiparticle term, the extrinsic and intrinsic loss satellites, and the interference between them. To handle the one-particle propagators  $g(\omega)$  we assume that  $\Sigma(\omega)$  is diagonal in a representation with eigenfunctions  $|k'\rangle$  of  $h'$  that according to calculations with the GW approximation for the self-energy, is not too bad.<sup>17</sup> For simplicity we now drop the prime on  $k'$  and write

$$\langle k | g(\omega) | k \rangle \equiv g(k, \omega) = \frac{1}{\omega - \varepsilon_k - \Sigma(k, \omega) + i\gamma}. \quad (33)$$

With  $k$  fixed  $\langle k | g(\omega) | k \rangle$  as a function of  $\omega$  has a quasiparticle peak and some more or less pronounced satellite structure. For  $\omega$  near the quasiparticle peak we obtain an asymmetric lineshape,

$$g(k, \omega) \approx \langle k | g_{\text{qp}}(\omega) | k \rangle = \frac{Z_k}{\omega - E_k + i\Gamma_k}, \quad (34)$$

where  $E_k$  is defined from  $E_k = k^2/2 + \text{Re} \Sigma(k, E_k)$ ,  $\Gamma_k = |\text{Im} \Sigma(k, E_k)|$  and  $Z_k = [1 - \partial \Sigma(k, \omega) / \partial \omega]_{\omega=E_k}^{-1}$ . We now make an on-shell approximation, defining functions of  $\omega$ ,

$$Z(\omega) = Z_k, \quad \Delta E(\omega) = \Delta E_k, \quad \Gamma(\omega) = \Gamma_k,$$

with the relation between  $k$  and  $\omega$  given implicitly through

$$\omega = E_k. \quad (35)$$

Strictly speaking  $\Sigma$  is defined from  $h + \Sigma = t + V_H + \Sigma$ , where  $t$  is the kinetic energy and  $V_H$  the Hartree potential. Often we would like to use, e.g.,  $V_{\text{LDA}}$  rather than  $V_H$  to generate basis functions. We then have to replace  $\Sigma$  by  $\Sigma - V_{\text{LDA}} + V_H$  in our expressions. With this on-shell approximation we have

$$\langle k | g_{\text{qp}}(\omega) | k \rangle \approx \left\langle k \left| \frac{Z(\omega)}{\omega - h' - \Delta E(\omega) + i\Gamma(\omega) + i\gamma} \right| k \right\rangle, \quad (36)$$

and since the  $|k\rangle$  are eigenfunctions of  $h'$ , the operator  $g_{\text{qp}}(\omega)$  becomes

$$g_{\text{qp}}(\omega) = \frac{Z(\omega)}{\omega - h' - \Delta E(\omega) + i\Gamma(\omega) + i\gamma}. \quad (37)$$

With this form for the quasiparticle propagator  $g_{\text{qp}}(\omega)$  we can use the MS expansion to treat the XAFS.<sup>10</sup> We write  $h' = t + V'_0 + V_{\text{scatt}}$  where  $t$  is the kinetic-energy operator,  $V'_0$  the potential in the central cell with its core hole, and  $V_{\text{scatt}}$  the total scattering potential from all the neighboring cells (excluding inelastic losses). In the MS expansion we can, e.g., use  $h_0 = t + V'_0 - i\Gamma(\omega) - i\gamma$  to obtain the propagator for the central absorber and then treat  $V_{\text{scatt}}$  as the perturbation.

From Eqs. (31) and (32), the quasiparticle contribution to the x-ray absorption is

$$\mu_{\text{qp}}(\omega) = -\frac{e^{-a}}{\pi} \text{Im} \langle b | d^\dagger P g_{\text{qp}}(\omega) P d | b \rangle, \quad (38)$$

where the propagator  $g_{\text{qp}}(\omega)$  is given by Eq. (37). This is similar to the standard one-electron formula for the x-ray absorption  $\mu^{(1)}(\omega)$  with mean-free-path effects from the damping parameter  $\Gamma(\omega)$ , except for a complex amplitude factor  $Z(\omega) = \exp(i\phi)|Z(\omega)|$  with a many-body phase shift  $\phi$  and a wave-function overlap reduction by the factor  $e^{-a}$ . With  $\Gamma$  and  $a$  both zero and  $Z=1$ , the quasiparticle XAS  $\mu_{\text{qp}}(\omega)$  becomes identical to the one-particle absorption  $\mu^{(1)}(\omega)$  in Eq. (22).

To evaluate the total absorption  $\mu(\omega)$  including intrinsic losses and interference, we can, correct to terms of second order in the fluctuation potentials  $V^n$ , replace  $g(\omega)$  by  $g_{\text{qp}}(\omega)$  in  $g_{\text{intr}}(\omega)$  and  $g_{\text{inter}}(\omega)$ . For definiteness we define the extrinsic satellite function  $g_{\text{extr}}(\omega)$  as the difference between the full propagator  $g(\omega)$  and the quasiparticle propagator  $g_{\text{qp}}(\omega)$  (see Appendix A). As noted above, the projection operator  $P$  in Eq. (31) and Eq. (22) is necessary to account for edge singularity effects, but does not significantly affect the fine structure. In Appendix A we also show that the many-body expression for the x-ray absorption  $\mu(\omega)$  can be expressed as a convolution of an effective spectral function  $A_{\text{eff}}(\omega, \omega')$ , and the quasiparticle absorption  $\mu_{\text{qp}}$  from Eq. (38), i.e.,

$$\mu(\omega - E_c) = \int d\omega' A_{\text{eff}}(\omega, \omega') \mu_{\text{qp}}(\omega - \omega'), \quad (39)$$

where  $\omega'$  is the excitation energy.

To evaluate our theory numerically in real systems is a heavy undertaking, and we will here only carry out some rough estimates that illustrate the theory and yield non-negligible corrections to the usual XAFS procedure.<sup>10</sup> To simplify these calculations we rely on electron-gas theory within the plasmon-pole approximation to evaluate the various contributions to the effective spectral function, and then use these results to estimate the corresponding contributions to  $\mu(\omega)$ . Since our aim here is only to carry out a pilot study, which is at best semiquantitative, such an approximate model seems appropriate. However, our approach is more general, and could be refined at the expense of much heavier calculations.

### III. MODEL CALCULATIONS

In this section we present electron-gas model calculations based on the plasmon-pole approximation (Appendix B) for the various contributions to the effective spectral function  $A_{\text{eff}}$ . They can be represented as a sum of quasiparticle, interference, intrinsic, and extrinsic satellite terms defined in Appendix A, i.e.,

$$A_{\text{eff}}(\omega, \omega') = [1 + 2a(\omega)] \delta(\omega') + A^{\text{sat}}(\omega, \omega'), \quad (40)$$

where

$$A^{\text{sat}}(\omega, \omega') = A_{\text{extr}}(\omega, \omega') + A_{\text{intr}}(\omega, \omega') - 2A_{\text{inter}}^{\text{sat}}(\omega, \omega'). \quad (41)$$

Since we make comparisons to XAFS experiments for fcc Cu metal, we have set  $r_s = 1.80$ , that corresponds to the mean interstitial electron density. For this density, the dimensionless constant  $a$  relating the strength of the electron-plasmon coupling to the plasmon excitation energy is 0.31. Near threshold the net weight of each of the contributions  $A_{\text{extr}}$ ,  $A_{\text{inter}}^{\text{sat}}$  and  $A_{\text{intr}}$  is equal to  $a$  and their shapes are similar, so that the sum of all of these contributions tend to cancel. Also near threshold,  $Z \approx \exp(-a)$  and the interference contribution to the quasiparticle peak  $a(\omega) \approx a$ . Thus the net strength of the main peak at threshold in our second-order theory is  $Z \exp(-a)(1+2a) \rightarrow 1 + O(a^2)$ .

As noted above, the asymmetric *quasiparticle* spectrum  $A_{\text{qp}}(k, \omega) = (-1/\pi) \text{Im} g_{\text{qp}}(k, \omega)$  [see Eq. (34)], gives rise to a net reduction in the XAFS amplitude as well as an additional phase shift compared to one-electron theory. These effects are due to the behavior of the complex renormalization constant  $Z(\omega)$ , which gives  $A(\omega)$  an asymmetric Fano lineshape. In Fig. 1 we plot the modified quasiparticle spectrum  $A_{\text{qp}}^{\text{mod}}(k, \omega)$ , where long-range contribution from the imaginary part of  $Z_k$  is cut off in  $A_{\text{qp}}^{\text{mod}}$  [cf. Appendix A and Eq. (A18)], i.e.,

$$A_{\text{qp}}^{\text{mod}}(k, \omega + E_k) = \frac{1}{\pi} \frac{\Gamma_k \text{Re} Z_k - \omega e^{-(\omega/2\omega_p)} \text{Im} Z_k}{\omega^2 + \Gamma_k^2}. \quad (42)$$

For comparison, we also show the total extrinsic spectral function including both quasiparticle and satellite parts. Note that  $A_{\text{qp}}^{\text{mod}}(k, \omega)$  has nothing to do with the different contri-

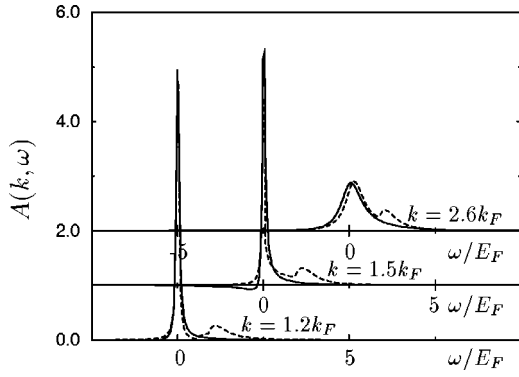


FIG. 1. Quasiparticle spectral function  $A_{\text{qp}}^{\text{mod}}(k, \omega + E_k)$  in Eq. (42) plotted vs  $\omega$  for different values of the wave number  $k$  (solid line); and the spectral function [cf. Eq. (33)]  $(-1/\pi)\text{Im } g$  (dashed line). All parameters are calculated using a plasmon-pole dielectric function for an electron gas at the mean interstitial electron density in Cu  $r_s = 1.80$ .

contributions to  $A_{\text{eff}}$ . The real and imaginary parts of the renormalization constant  $Z(\omega)$  are plotted in Fig. 2.

The *intrinsic contribution*  $A_{\text{intr}}(\omega, \omega')$  to  $A_{\text{eff}}(\omega, \omega')$  is independent of  $\omega$  and gives a well-defined satellite structure peaking at an energy  $\omega_p$  away from the quasiparticle (Fig. 3). Although  $A_{\text{intr}}$  turns on sharply, this singular structure is suppressed by broadening and interference terms as described below. The *interference* between extrinsic and intrinsic losses results in a net shift of spectral weight away from the satellite and to the quasiparticle peak, overall spectral weight being conserved. The rough cancellation of the satellite terms due to interference is clearly illustrated by the behavior of  $A_{\text{inter}}^{\text{sat}}$  in Fig. 3. Note that the interference satellite amplitude is maximal near threshold and slowly decreases with increasing energy over a range of several  $\omega_p$ .

The behavior of the extrinsic satellite spectral function is illustrated in Fig. 4. In the plasmon-pole, electron gas model used here, the *extrinsic satellite* spectral function sometimes

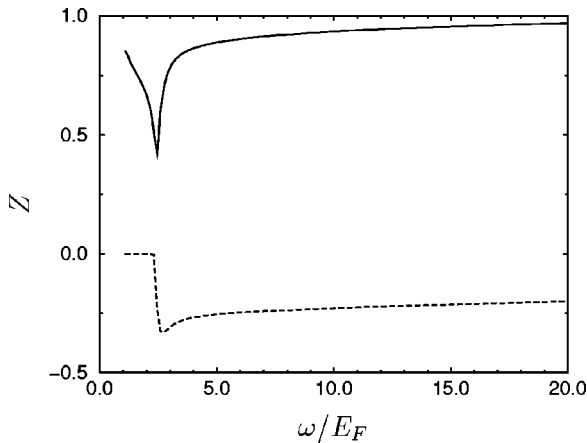


FIG. 2. Real (solid line) and imaginary (dashed) parts of the quasiparticle renormalization constant  $Z(\omega) = 1/(1 - \partial\Sigma/\partial\omega)$ , calculated at the quasiparticle peak, for the GW plasmon-pole self-energy  $\Sigma$  of an electron gas at  $r_s = 1.80$ . The sharp structure occurs at the onset of plasmon excitations.

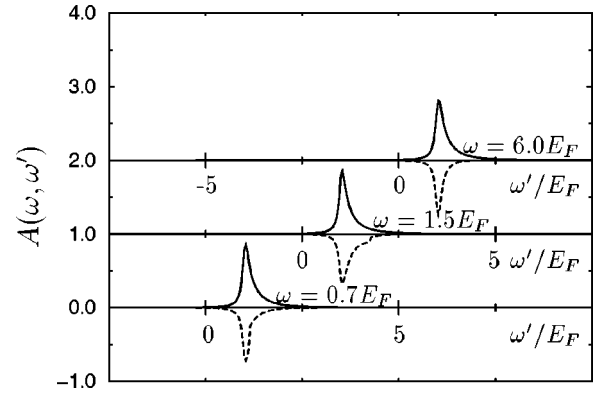


FIG. 3. Intrinsic (solid line) and interference satellite (dashed) spectral functions  $A_{\text{intr}}(\omega, \omega')$  and  $A_{\text{inter}}^{\text{sat}}(\omega, \omega')$ , plotted against  $\omega'$  for selected values of  $\omega$ . Note that the interference contribution is negative and tends to cancel the intrinsic satellite. These quantities are both calculated using the plasmon-pole dielectric function for an electron gas at density  $r_s = 1.80$ , and broadened by a Lorentzian of width  $0.2\omega_p$ .

exhibits a complicated structure. Close to the Fermi energy, the structure simplifies and consists of a peak at an energy about  $\omega_p$  above the quasiparticle energy  $\omega$  and a smooth structure that falls off gradually with increasing energy. For  $\omega$  near the onset of plasmon losses, there is still a pronounced satellite peak, but there is also an additional “anomalous” structure near the quasiparticle energy. Indeed, it seems ambiguous whether the structure close to the quasiparticle energy should be considered as part of the satellite or the main peak, as the structure accounts for a substantial portion of the extrinsic weight  $[1 - Z(\omega)]$  that is not included in the quasiparticle peak. This indicates that the anomalously low and singular behavior of  $Z(\omega)$  in this region is partly due to the singular structure of the plasmon-pole approximation and largely an artifact of the *ad hoc* method used to separate the main peak and the “satellite” spectral function. Above the onset of plasmon losses, the

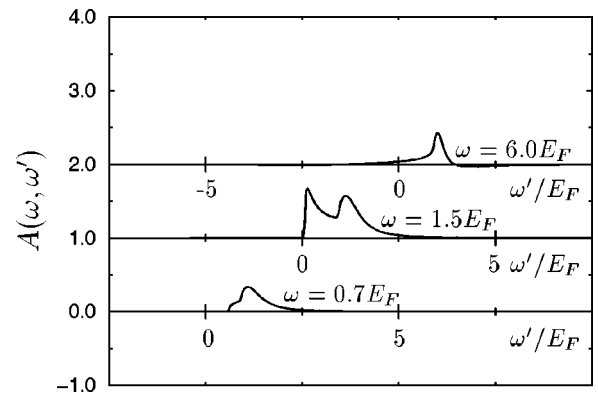


FIG. 4. Extrinsic satellite spectral function  $A_{\text{extr}}(\omega, \omega')$  obtained as described in Appendix A for selected values of  $\omega_i$  vs  $\omega'$ . The curve for  $\omega = 0.7E_F$  and  $\omega = 1.5E_F$  lie before the onset of plasmon excitations. The result for  $\omega = 1.5E_F$  illustrates the anomalous structure seen in this region, and that for  $\omega = 6E_F$  lies well beyond the onset. All results are based on a plasmon-pole dielectric function with  $r_s = 1.80$ .

anomalous structure disappears, and is replaced by a small tail that extends to the vicinity of the quasiparticle peak. Moreover, as the quasiparticle energy increases, the extrinsic satellite weight becomes progressively smaller.

#### IV. IMPLICATIONS FOR XAFS

We can now obtain rough estimates for the effect of extrinsic and intrinsic losses and interference on the XAFS spectrum. In the usual MS theory,<sup>10</sup> the XAFS spectrum  $\chi^{(1)}(\omega)$  is a rapidly varying energy dependent factor in the one-particle expression for the x-ray absorption,

$$\mu^{(1)}(\omega) = \mu_0^{(1)}(\omega)[1 + \chi^{(1)}(\omega)], \quad (43)$$

where  $\mu_0^{(1)}$  is the generally smooth absorption from the central atom alone, in the absence of MS. The conventional (broadened) one-particle absorption  $\mu^{(1)}(\omega)$  is obtained from Eq. (12), with  $g_{\text{eff}}(\omega) = 1/[\omega - h - i\Gamma(\omega)]$ , i.e., with a damped one-particle propagator with mean-free-path effects taken into account in terms of  $\Gamma(\omega)$ . This one-particle MS theory is generally in good agreement with experiment. However, there remains a residual discrepancy of about 10% in overall XAFS amplitudes and a systematic shift in peak positions compared to experiment. This shift is only partly accounted for by including the real part of an electron-gas self-energy in the one-particle propagator.

In the present theory, the many-body effects of losses and interference can be represented as in Eq. (39), i.e., as a convolution of  $\mu_{\text{qp}}(\omega)$  with the effective spectral function  $A_{\text{eff}}(\omega, \omega')$  including contributions from both primary and satellite channels, as discussed in Appendix A. As noted above, the difference between the behavior of  $\mu^{(1)}(\omega)$  and  $\mu_{\text{qp}}(\omega)$  is qualitatively minor and results primarily from a constant wave function overlap factor  $\exp(-a)$ , a complex renormalization factor  $Z(\omega) = |Z(\omega)|\exp(i\phi)$ , and an energy shift  $\Delta E(\omega)$ . The phasefactor  $\phi$  can be absorbed by adding  $\phi/2$  to the central atom phase factor in the XAFS formula.

To extract the XAFS  $\chi(\omega)$  corrected for many-body effects, we first use a similar MS factorization of  $\mu_{\text{qp}}(\omega) = \mu_{\text{qp}}^0[1 + \chi_{\text{qp}}(\omega)]$  to split off a central cell contribution  $\mu_{\text{qp}}^0(\omega)$ , which yields a many-body expression for the atomic background absorption

$$\begin{aligned} \mu_0(\omega) &= \int d\omega' A_{\text{eff}}(\omega, \omega') \mu_{\text{qp}}^0(\omega - \omega') \\ &\approx \mu_{\text{qp}}^0(\omega) \int_{-\infty}^{\omega - E_F} d\omega' A_{\text{eff}}(\omega, \omega'). \end{aligned} \quad (44)$$

Here  $\mu_{\text{qp}}^0(\omega) \sim |\langle \phi_k^{\text{qp}} | P d | b \rangle|^2$  is the absorption from the central atom alone, in the absence of other scatterers, and we have neglected the variation of  $\mu_{\text{qp}}^0(\omega)$  over the dominant integration range of  $\omega'$ . This is usually a good approximation, since the one-particle atomic background is usually a smooth, monotonically decreasing function of energy. Thus one expects that the satellite structure in the spectral function due to many-body excitations will generally have minor effects on  $\mu_0(\omega)$ , which is consistent with experimental observations. However, the existence of sharp atomic reso-

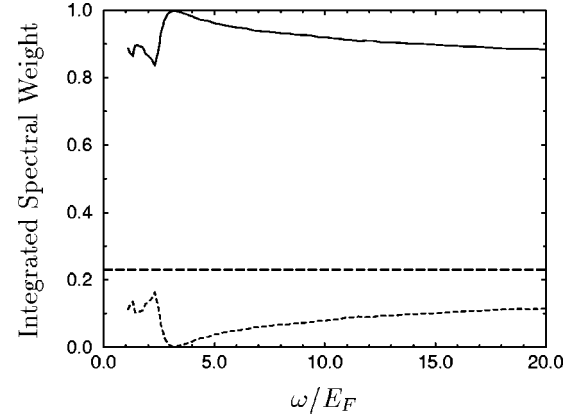


FIG. 5. Normalized total spectral weights of the net primary peak (solid) and satellite terms (dashed) including interference, i.e., the integrated quantities  $\bar{a}^{\text{sat}}(\omega)$  and  $\bar{a}_0(\omega)$  of Eq. (47) and Eq. (48). The anomalous structure at low energies is an artifact of the method used to separate primary and satellite terms in the spectral function. All results are obtained for the model of this paper with  $r_s = 1.80$ . The horizontal line represents the high-energy limit of the satellite weight (i.e., the sudden approximation).

nances in the one-particle absorption  $\mu_{\text{qp}}^0$  may lead to exceptions. The many-body XAFS function  $\chi(\omega) = (\mu - \mu_0)/\mu_0$  then becomes

$$\chi(\omega) \approx \int d\omega' \tilde{A}_{\text{eff}}(\omega, \omega') \chi_{\text{qp}}(\omega - \omega'), \quad (45)$$

where the spectral function  $\tilde{A}_{\text{eff}}$  is now normalized to unity,

$$\tilde{A}_{\text{eff}}(\omega, \omega') = A_{\text{eff}}(\omega, \omega')/N(\omega), \quad (46)$$

and  $N(\omega) = \int d\omega' A_{\text{eff}}(\omega, \omega')$ . With this normalization in  $\chi(\omega)$ , the wave function renormalization factor  $\exp(-a)$  and the magnitude of the quasiparticle strength  $|Z|$  cancel out, while the phase  $\phi$  and the energy shift  $\Delta E(\omega)$  both remain.

The importance of multielectron excitations can be gauged by the net spectral weight in main peak and in the satellite structure from all losses. A plot of the normalized integrated satellite spectral weight,

$$\bar{a}^{\text{sat}}(\omega) = \int d\omega' \tilde{A}^{\text{sat}}(\omega, \omega'), \quad (47)$$

where  $\tilde{A}^{\text{sat}}(\omega, \omega') = A^{\text{sat}}/N(\omega)$  is given in Fig. 5. Also plotted is the total weight of the primary peak,

$$\bar{a}_0(\omega) = [1 + 2a(\omega)]/N(\omega). \quad (48)$$

Note, in particular, the slow trend of the satellite weight towards the sudden approximation limit  $[a \exp(-a)]$  with increasing energy over a range of a few hundred eV. In these plots we have lumped the contributions to the spectral function that lie below the plasmon onset into the primary peak. The anomalous behavior of the weights near the plasmon onset energy is due to the ambiguity of separating the satellite and quasiparticle contributions, and does not lead to singular structure in the overall absorption.

The net effect of the convolution over a normalized, positive spectral amplitude  $\tilde{A}_{\text{eff}}(\omega, \omega')$  of Eq. (45) is clearly a decreased XAFS amplitude and a phase-shifted oscillatory signal compared to the one-particle XAFS  $\chi^{(1)}$ . In the single scattering approximation the oscillatory energy dependence of  $\chi_{\text{qp}}(\omega)$  enters primarily through the complex exponential  $\exp[i2k(\omega)R]$ , where  $R$  is an interatomic distance and  $k(\omega) = \sqrt{2(\omega - E_F)}$  is the photoelectron wave vector. The result of the convolution can be written in terms of a complex amplitude factor  $S_0^2(\omega, R) = |S_0^2(\omega, R)| \exp(i\Phi(\omega, R))$ , which is given by an energy dependent ‘‘phasor sum’’ over the effective normalized spectral function,

$$S_0^2(\omega, R) = \int_0^\omega d\omega' \tilde{A}_{\text{eff}}(\omega, \omega') \exp\{i2[k(\omega - \omega') - k(\omega)]R\}. \quad (49)$$

The qualitative behavior of  $S_0^2(\omega, R)$  can be understood as follows: At very low energies compared with the excitation energy  $\omega_p$ , the satellite terms strongly cancel so  $A(\omega, \omega') \approx \delta(\omega - \omega')$  and hence,  $S_0^2(\omega, R) \rightarrow 1$ . At high energies, the sudden approximation prevails, and  $A \approx A_{\text{qp}} + A_{\text{intr}}$ , which has a strong satellite structure. However, the phase difference  $2[k(\omega - \omega') - k(\omega)]$  between the primary channel and satellite becomes small at high energies ( $\omega' \gg \omega_p$ ) and hence also  $S_0^2(\omega, R) \rightarrow 1$ . At intermediate energies, however, the value of  $S_0^2(\omega, R)$  has a minimum. A plot of the magnitude and phase of  $S_0^2(\omega, R)$  for our electron-gas model is given in Fig. 6, for the first neighbor distance of Cu metal  $R = 2.55 \text{ \AA}$ .

In order to compare these results with experiment, we isolate the first shell of the experimental EXAFS signal  $\chi(\omega, R)$  by Fourier filtering over the range  $1.75 < R < 2.80 \text{ \AA}$  in position-space  $R$  (conjugate to  $2k$ ), with a smooth sine window, and then back transforming to  $k$  space. For this comparison, we use the usual EXAFS convention for the wave number  $k = \sqrt{2(E - E_F)}$ , as measured from the threshold Fermi energy. Our estimate of the experimental  $S_0^2(\omega, R)$  is then given by the ratio of this back-transformed experimental first-shell XAFS signal  $\chi(\omega, R)$  to a similarly Fourier filtered and back-transformed theoretical first-shell signal  $\tilde{\chi}^{(1)}(\omega, R)$ . The latter is obtained from *ab initio* XAFS calculations using the FEFF8 code.<sup>18</sup> The FEFF8 calculations include only extrinsic losses, i.e., the mean-free-path loss calculated from a Hedin-Lundqvist plasmon-pole self-energy model. The results, from both theory and experiment are also plotted in Fig. 6. Due to the Fourier filtering, fine details of the theoretical phasor sum for  $S_0^2(\omega, R)$  in Fig. 6, are lost. Also plotted, in Fig. 6, is the back-transformed XAFS amplitude  $|\tilde{\chi}^{(1)}(\omega(k), R)|$  for the first nearest neighbor of Cu. This illustrates both where the amplitude reduction is important in analysis, and also where  $\chi$  is small, and hence the  $S_0^2(\omega, R)$  extracted from experiment may have significant errors due to experimental noise. Given the rough, electron-gas approximations used in our model calculations, the overall agreement with experiment for Cu metal is reasonably good. This result also suggests that the conventional procedure of approximating  $S_0^2(\omega, R)$  by a constant  $S_0^2 \approx 0.9$  is not unreason-

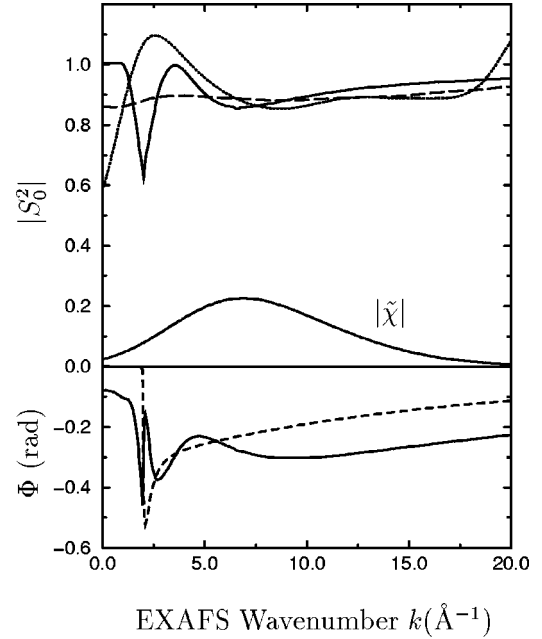


FIG. 6. Upper curves: magnitude  $|S_0^2|$  (solid) of the XAFS many-body amplitude reduction factor due to all inelastic losses, as calculated using a phasor summation over the total spectral function for the model in this work, and plotted vs the EXAFS wave number  $k = \sqrt{2(\omega - E_F)}$  for the first neighbor distance  $R = 2.55 \text{ \AA}$  in Cu. Shown for comparison are the experimental (dots) and theoretical (dashes) amplitude reduction obtained by Fourier filtering (see text). Note that the largest discrepancy between theory and experiment occurs where  $|\tilde{\chi}^{(1)}(k, R)|$ , the Fourier filtered and back-transformed complex XAFS amplitude, is small and experimental noise dominates. Lower curves: phase  $\Phi$  of  $S_0^2(k, R)$  (solid), and comparison, the many body phase shift of the asymmetric quasiparticle peak (dashes), i.e.,  $\phi = \tan^{-1}[\text{Im} Z / \text{Re} Z]$ . The sharp structure near  $k \approx 2$  is an artifact of the sudden plasmon onset in the plasmon pole model used here.

able. The biggest discrepancies are at low energies, and are likely due both to experimental noise and to the approximation used for the mean-free-path at low energies in FEFF8, which often has too much loss. We have also plotted the many-body correction to the XAFS phase, which varies by about  $+0.2$  radians over the XAFS experimental range  $3 < k < 20 \text{ \AA}^{-1}$ . By comparing with the phase of the renormalization constant  $Z$  (Fig. 2), one sees that much of the phase shift arises from the asymmetry of the quasiparticle peak. The sign of the phase shift is consistent with a reduction in the strength of the self-energy due to cancellation effects. The approximate linear variation of the phase with  $k$  can lead to errors in distance determinations from XAFS measurements of about  $\delta R = \Delta\Phi / 2\Delta k \approx +0.006 \text{ \AA}$  which is comparable to systematic errors typically encountered in experimental XAFS analysis.

Finally, we plot in Fig. 7 a comparison with experiment of the full absorption result  $\mu(\omega)$  obtained by convoluting the spectral function  $A_{\text{eff}}$  with the quasiparticle result  $\mu_{\text{qp}}(\omega)$ . These calculations were carried out using full-multiple scattering calculations for a cluster of 300 Cu atoms using the FEFF8 code. To compensate for errors in our second-order

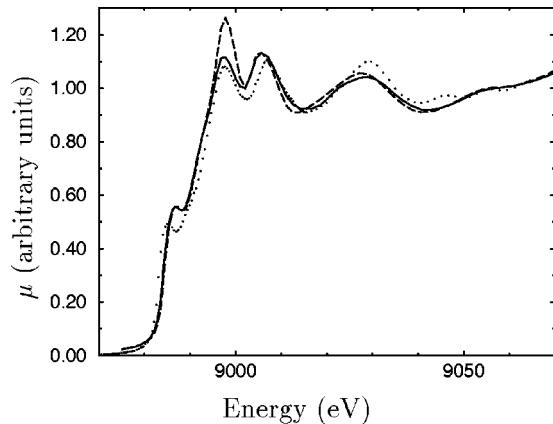


FIG. 7. Comparison of the full calculated many-body XAS  $\mu(\omega)$  (solid) obtained by convoluting the spectral function  $A_{\text{eff}}$  for the model of this paper with the one-particle XAS  $\mu^{(1)}(\omega)$  (dashes) calculated using the FEFF8 code, and the result from Cu experiment (dots).

expression for the spectral function,  $A_{\text{eff}}$  was normalized to unity in this convolution; also since  $\mu_{\text{qp}}$  is real, the asymmetry in the quasiparticle peak in Eq. (42) was represented by a term  $P \text{Im}Z/\omega$  (where  $P$  denotes the principal part) rather than a complex phase factor  $\exp i\phi$ . Although it is not clear how reliable such a calculation is at the edge, given the simplicity of our model calculations, the agreement with experiment does markedly improve.

## V. CONCLUDING REMARKS

We have developed a semiquantitative theory for the effects of extrinsic and intrinsic losses and the interference between them on x-ray absorption spectra. The theory is based on a quasiboson representation for the excitations, and perturbation theory to second order in the electron-boson coupling. These losses lead to an asymmetric broadening of the main quasiparticle peak, plus a broad energy-dependent satellite in the spectral function due to the boson excitation. We find that the interference terms strongly suppress the satellite terms and enhance the main quasiparticle peak. These results thereby explain the general weakness of multielectron excitations in XAS. We have applied the theory within the electron-gas approximation to estimate the many-body corrections to the XAFS. By using a phasor summation over the spectral function, the theory yields an approximation to the reduction in the XAFS amplitude beyond the usual extrinsic, mean-free path, together with an additional many-body phase shift. Pilot model calculations based on the electron-gas approximation and our formalism are in semiquantitative agreement with XAFS experiment.

Our results illustrate a striking difference with those for losses in photoemission. In core electron photoemission for metals there is also a strong extrinsic contribution to the losses for all energies, and a strong interference effect between extrinsic and intrinsic losses up to energies in the keV region.<sup>16</sup> In contrast, we found the extrinsic losses to have a very small influence on XAS. This at first seems to be a paradox, since photoabsorption is usually considered to be

proportional to the photoyield. This is indeed true in one-electron theory, and is also observed to be approximately true experimentally in many cases. There is, however, no theoretical justification for assuming this to be the case in general. If we examine the problem formally, the XAS is related to the dielectric response function (i.e., the density-density correlation function), while the PES is given by a three-current correlation function, and there are no simple connections between these quantities. More physically we can point at the fact that in PES we measure a sharp, well-defined photoelectron; i.e., we can describe PES by the golden rule with well-defined final states. In XAS the photoelectrons are never measured, and photoelectron states are not sharp, they are decaying states with a finite lifetime. Further all electrons that are photoexcited do not leave the solid, and some PES current that leaves the solid is due to secondary electrons that cannot come back and interfere at the photoexcited atom. We never consider these secondary electrons since we do not allow our quasibosons to decay. If we could put in well-defined intermediate states with a photoelectron in the density-density correlation function we would indeed have the same matrix elements that enter in PES but that is not possible except perhaps approximately, very close to threshold when the quasiparticle lifetime is long.

Finally we would like to comment on similarities and difference between our approach and a model studied by Schrieffer.<sup>19</sup> That work considered an Anderson-Newns-like model for PES from a valence level on an adsorbed atom, coupled to surface plasmons. Schrieffer studied photoabsorption, and by cutting the polarization diagram, he identified a PES final state and obtained a perfect-square expression for the PES current, including interference effects. His results agree precisely with what we have in our model both for XAS and when applied to PES. However, the results for XAS cannot be expressed as a perfect square, as needed to have a close correspondence with PES. This is due to the differences in the signs of the imaginary parts, as can be seen by comparing Eqs. (7), (13), and (14a) in Ref. 19. Thus photoabsorption and photoyield are only approximately related, even for a finite system where the quasiparticle aspect does not enter.

## ACKNOWLEDGMENTS

We thank T. Fujikawa for useful remarks and G. Strinati for critical comments long ago when two of us (W.B. and L.H.) started thinking about this problem. This work was supported in part by DOE Grant DE-FG03-97ER45623/A000 (L.W.C. and J.J.R.).

## APPENDIX A: DERIVATION OF THE EFFECTIVE SPECTRAL FUNCTION

In this appendix we derive expressions for the different parts in the spectral weight function  $A_{\text{eff}} \equiv A_{\text{qp}} + A_{\text{extr}} + A_{\text{intr}} + A_{\text{inter}}$  that appears in the convolution expression for the x-ray absorption in Eq. (39). Starting from Eq. (31), we have

$$\mu(\omega - E_c) = -\frac{e^{-a}}{\pi} \sum_k |\langle b|d^\dagger P|k\rangle|^2 \text{Im} g_{\text{eff}}(k, \omega), \quad (\text{A1})$$

provided  $g_{\text{eff}}$  [see Eq. (32)] is diagonal in the one-particle index  $k$ . From GW calculations we know that  $g$  and  $g_{\text{qp}}$  are approximately diagonal,<sup>17</sup> and this is hence a reasonable approximation for all contributions to  $g_{\text{eff}}$  except  $g_{\text{inter}}$ , which requires a special treatment as described later in this appendix. We first introduce the real spectral weight function  $A_{\text{eff}}(k, \omega)$  by representing  $\text{Im} g_{\text{eff}}(k, \omega)$  as

$$\text{Im} g_{\text{eff}}(k, \omega) = \int d\omega' A_{\text{eff}}(k, \omega') \text{Im} g_{\text{qp}}(k, \omega - \omega'). \quad (\text{A2})$$

Next we make the on-shell approximation of replacing  $k$  in  $A_{\text{eff}}(k, \omega')$  by  $k = k(\omega - \omega')$ , with  $k(\omega)$  defined in Eq. (35). With  $A_{\text{eff}}(\omega, \omega') \equiv A_{\text{eff}}(k(\omega - \omega'), \omega')$  depending only on  $\omega$  and  $\omega'$ , we can perform the summation over  $k$ , and obtain

$$\mu(\omega - E_c) = \int d\omega' A_{\text{eff}}(\omega, \omega') \mu_{\text{qp}}(\omega - \omega'), \quad (\text{A3})$$

where  $\mu_{\text{qp}}(\omega)$  is defined in Eq. (38). Thus the quasi-particle contribution to  $A_{\text{eff}}(\omega, \omega')$  is simply a delta function,  $A_{\text{qp}}(\omega, \omega') = \delta(\omega')$ .

For the *intrinsic contribution*, it is clear from Eq. (32) that  $A_{\text{intr}}$  is simply a sum of energy-shifted  $\delta$  functions,

$$A_{\text{intr}}(\omega, \omega') = \sum_n \left( \frac{V_{bb}^n}{\omega_n} \right)^2 \delta(\omega' - \omega_n), \quad (\text{A4})$$

which is independent of  $\omega$ . In the electron-gas, plasmon-pole approximation the explicit expression for  $A_{\text{intr}}$  can easily be found (Ref. 14, p. 655),

$$A_{\text{intr}}(\omega, \omega') = \frac{\omega_p^2 \theta(\omega' - \omega_p)}{\pi(\omega')^3 q(\omega')}, \quad (\text{A5})$$

where  $q(\omega')$  is a solution to  $\omega_q = \omega'$ . The intrinsic spectral function contributes only at energies near  $\omega_p$  above the electron quasiparticle energy, and gives a well-defined satellite.

The *interference contribution* to  $g_{\text{eff}}$  in Eq. (32) contains a product  $g(\omega - \omega_n) V^n g(\omega)$ , and since  $V^n$  can transfer momentum, is not diagonal in  $k$  space even when  $g$  is. One can evaluate  $g_{\text{inter}}(\omega)$ , e.g., by doing MS expansions of the two propagators, but this does not yield a result of the form in Eq. (39). To force it into that form we make some further approximations. First we take the fluctuation potentials as plane waves, and in a plane wave basis we then have  $\langle k + q' | V^q | k \rangle = V_0^q \delta_{qq'}$ . Also taking the Green's functions as diagonal in a plane wave basis, Eqs. (31) and (32) give

$$\begin{aligned} \mu_{\text{inter}}(\omega) &= \frac{2e^{-a}}{\pi} \text{Im} \sum_{kq} \frac{|V_0^q|^2}{\omega_q} \langle b | d^\dagger P | k + q \rangle \\ &\quad \times \langle k + q | g(\omega - \omega_q) | k + q \rangle \langle k | g(\omega) | k \rangle \langle k | P d | b \rangle. \end{aligned} \quad (\text{A6})$$

Taking the quasiparticle approximation in Eq. (34) for  $g(\omega)$  and neglecting the  $q$ -dependence in the dipole-matrix element, we have

$$\begin{aligned} \mu_{\text{inter}}(\omega) &= \frac{2e^{-a}}{\pi} \text{Im} \sum_{kq} \frac{|V_0^q|^2}{\omega_q} |\langle k | P d | b \rangle|^2 \frac{Z_{k+q} Z_k}{\omega_q + E_{k+q} - E_k} \\ &\quad \times \left[ \frac{1}{\omega - \omega_q - E_{k+q} + i\Gamma_{k+q}} - \frac{1}{\omega - E_k + i\Gamma_k} \right], \end{aligned} \quad (\text{A7})$$

where we have made the approximation that  $\Gamma_{k+q} \approx \Gamma_k$  in the denominator of the prefactor before the term in brackets. We now have a difference between two Green's functions, and provided we treat the prefactor of this difference as a real number (e.g., neglecting the imaginary part of  $Z$ ) we can again write  $\mu_{\text{inter}}(\omega)$  as a convolution with  $\mu_{\text{qp}}$ , i.e.,

$$\begin{aligned} \mu_{\text{inter}}(\omega) &\approx 2 \left[ a(\omega) \mu_{\text{qp}}(\omega) - \int d\omega' A_{\text{inter}}^{\text{sat}}(\omega, \omega') \mu_{\text{qp}}(\omega - \omega') \right], \end{aligned} \quad (\text{A8})$$

with

$$a(\omega) = \sum_q \frac{|V_0^q|^2}{\omega_q} \frac{|Z_{k+q}|}{\omega_q + E_{k+q} - E_k} \Big|_{k=k(\omega)}, \quad (\text{A9})$$

$$\begin{aligned} A_{\text{inter}}^{\text{sat}}(\omega, \omega') &= \sum_q \frac{|V_0^q|^2}{\omega_q} \frac{|Z_{k-q}|}{\omega_q + E_k - E_{k-q}} \Big|_{k=k(\omega - \omega')} \\ &\quad \times \delta(\omega' - \omega_q). \end{aligned} \quad (\text{A10})$$

To further simplify the calculations, we assume that  $Z_{k+q} \approx Z_k$ . Thus we have separated the resulting spectral function into a term proportional to  $a(\omega)$  that adds to the quasiparticle peak, and a term proportional to  $A_{\text{inter}}^{\text{sat}}$  that contributes to the satellite structure. Approximating  $E_k$  by  $k^2/2$ , we obtain

$$a(\omega) = \frac{\omega_p^2 |Z_k|}{4\pi k} \int_0^\infty d\omega' \frac{1}{\omega' \omega_q^2} \ln \left[ \frac{\omega_q + \omega' + kq}{\omega_q + \omega' - kq} \right], \quad (\text{A11})$$

where  $q = \sqrt{2\omega'}$  and  $k = \sqrt{2\omega}$ . Similarly

$$\begin{aligned} A_{\text{inter}}^{\text{sat}}(\omega, \omega') &= \frac{|Z_{k'}| \omega_p^2}{2\pi k' q^2 \omega'^2} \\ &\quad \times \ln \left[ \frac{\omega' - q^2/2 + k'q}{\omega' - q^2/2 - k'q} \right] \theta(\omega' - \omega_p), \end{aligned} \quad (\text{A12})$$

where  $q = \sqrt{2(\omega' - \omega_p)}$  and  $k' = \sqrt{2(\omega - \omega')}$ .

For the *extrinsic contribution*, we have from Eq. (A2),

$$\text{Im} \left[ \frac{g_{\text{extr}}(k, \omega)}{Z_k} - \int \frac{A_{\text{extr}}(k, \omega') d\omega'}{\omega - \omega' - E_k + i\Gamma_k} \right] = 0. \quad (\text{A13})$$

The integral gives an analytic function of  $\omega$  in the half-plane above the line  $\omega = E_k - i\Gamma_k$ . If we also assume that  $g_{\text{extr}}(k, \omega) = g(k, \omega) - g_{\text{qp}}(k, \omega)$  is analytic in this region, we can make a shift in the origin for  $\omega$  by  $E_k - i\Gamma_k + i\delta$  ( $\delta \rightarrow 0^+$ ) without crossing the analyticity line. This gives

$$\text{Im} \left[ \frac{g_{\text{extr}}(k, \omega + E_k - i\Gamma_k + i\delta)}{Z_k} - \int A_{\text{extr}}(k, \omega') \frac{d\omega'}{\omega - \omega' + i\delta} \right] = 0, \quad (\text{A14})$$

from which we obtain

$$A_{\text{extr}}(k, \omega) = -\frac{1}{\pi} \text{Im} \left[ \frac{g_{\text{extr}}(k, \omega + E_k - i\Gamma_k + i\delta)}{Z_k} \right]. \quad (\text{A15})$$

The analyticity of  $g_{\text{extr}}(k, \omega)$  follows if it can be described by a sum of discrete poles or by a contour integration below  $\omega = E_k - i\Gamma_k$ . This is a reasonable approximation since the satellite peak is broader than the quasiparticle one. If for  $g_{\text{qp}}(k, \omega)$  we take the expression valid for  $\omega$  close to the quasiparticle energy

$$g_{\text{qp}}(k, \omega) = \frac{Z_k}{\omega - E_k + i\Gamma_k}, \quad (\text{A16})$$

and use it for all  $\omega$ , we have

$$g_{\text{extr}}(k, \omega) = \frac{1}{\omega - \varepsilon_k - \Sigma(k, \omega)} - \frac{Z_k}{\omega - E_k + i\Gamma_k}. \quad (\text{A17})$$

Since  $Z_k$  has a fairly large imaginary part, this leads to a substantial Fano-type asymmetry and substantial (cancelling) negative contributions in the spectral functions for  $g_{\text{extr}}$  and  $g_{\text{qp}}$ . The expression to use for  $g_{\text{qp}}$  is not well defined except very close to the quasiparticle energy. To avoid a negative spectral density for the extrinsic satellite we introduce a Gaussian cutoff to the imaginary part of  $Z_k$  in  $\text{Im} g_{\text{qp}}$ , i.e.,

$$\text{Im} g_{\text{qp}}(k, \omega + E_k - i\Gamma_k + i\delta) = \frac{-\delta \text{Re} Z_k + \omega e^{-(\omega/2\omega_p)^2} \text{Im} Z_k}{\omega^2 + \delta^2}. \quad (\text{A18})$$

If we further replace  $Z_k$  by  $|Z_k|$  in Eq. (A15), we obtain for  $\omega \gg \delta$

$$A_{\text{extr}}(k, \omega) = -\frac{1}{\pi |Z_k|} \left\{ [\Gamma_k + \text{Im} \Sigma(k, \omega + E_k)] \times 1 / [[\omega + \Delta E_k - \text{Re} \Sigma(k, \omega + E_k)]^2 + [\Gamma_k + \text{Im} \Sigma(k, \omega + E_k)]^2] - \frac{\text{Im} Z_k}{\omega} e^{-(\omega/2\omega_p)^2} \right\}, \quad (\text{A19})$$

where  $\Delta E_k = \text{Re} \Sigma(k, E_k)$ . We have neglected the  $i\Gamma_k$  in the argument for  $\Sigma$ , and we have only considered  $\omega \gg \delta$  since  $g_{\text{extr}}(k, \omega)$  is small around  $\omega = 0$  when the true complex quasiparticle energy is used. This result can be compared with the first-order result from Eq. (A2), i.e., the result obtained by

taking  $\Gamma_k \rightarrow 0$ . With  $\Gamma_k = 0$  and neglecting the phase in  $Z_k$  we have  $\text{Im} g_{\text{qp}}(k, \omega) = -\pi |Z_k| \delta(\omega - E_k)$ , and thus from Eq. (A2)  $A_{\text{extr}}(k, \omega - E_k) = -1/(\pi |Z_k|) \text{Im} g_{\text{extr}}(k, \omega)$ . This is the same result as in Eq. (A19) with  $\Gamma_k = 0$ . Since the GW approximation puts the extrinsic satellite at a slightly different position than the interference and intrinsic satellite terms, (which leads to numerical problems such as small regions where the spectral function is negative) we shifted  $A_{\text{extr}}$  to make the peaks coincide.

In summary we have found that

$$\mu(\omega - E_c) = \int d\omega' A_{\text{eff}}(\omega, \omega') \mu_{\text{qp}}(\omega - \omega'), \quad (\text{A20})$$

where

$$A_{\text{eff}}(\omega, \omega') = [1 + 2a(\omega)] \delta(\omega') + A_{\text{extr}}(\omega, \omega') + A_{\text{intr}}(\omega, \omega') - 2A_{\text{inter}}^{\text{sat}}(\omega, \omega'). \quad (\text{A21})$$

## APPENDIX B: PLASMON-POLE, ELECTRON-GAS MODEL

In this appendix, we briefly outline some properties of the electron-gas model used in our calculations. In order to estimate the many-body effects on XAFS spectra, we need to make some simplifying approximations. By choosing to work with an electron-gas model, many of the formulas in our model can be found analytically, greatly simplifying the calculations. We further choose to use a plasmon-pole dielectric function. Although the model exhibits some nonphysical singular structure and no loss at low energies, it nevertheless gives mean-free paths and self-energy shifts in reasonable agreement with experiment. Under this approximation, the fluctuating potentials  $V^n$  are plane waves

$$V^n(\mathbf{r}) = V^q(\mathbf{r}) = V_0^q e^{i\mathbf{q}\cdot\mathbf{r}}.$$

In the case of coupling to the core hole (at  $\mathbf{r} = 0$ ) this yields  $V_{bb}^q = V_0^q$ . According to the plasmon-pole model<sup>20</sup>

$$V_0^q = \left( \frac{2\pi e^2 \omega_p^2}{q^2 \omega_q \Omega} \right)^{1/2}, \quad (\text{B1})$$

where  $\Omega$  is the system volume. For the case when the plasmon dispersion has the form  $\omega_q^2 = \omega_p^2 + \alpha q^2 + q^4/4$ , the imaginary part of  $\Sigma_{\text{GW}}(k, \omega)$  can be obtained analytically, i.e.,

$$\text{Im} \Sigma(k, \omega) = -\frac{\omega_p}{4k} \ln \left[ \frac{q_2^2}{\omega_p + q_2^2} \frac{\omega_p + q_1^2}{q_1^2} \right] \theta(\omega - \omega_{\text{th}}), \quad (\text{B2})$$

where  $\omega_{\text{th}}$  is the threshold for plasmon excitation, and  $q_1$  and  $q_2$  are limiting values of the inequalities  $\omega_q + (q-k)^2/2 - \omega < 0$  and  $\omega_q + (q+k)^2/2 - \omega > 0$ , and hence are solutions to a cubic equation,

$$kq^3 + \left( \omega + \alpha - \frac{3}{2}k^2 \right) q^2 + (k^3 - 2\omega k)q + \left( \omega_p^2 - \omega^2 + \omega k^2 - \frac{k^4}{4} \right) = 0, \quad (\text{B3})$$

with the constraints,  $\min(q_1, q_2) = 0$ , and  $\max(q_1, q_2) = 0$  satisfies  $\omega_q = \omega + k^2/2 - k_F^2/2$ . The real part is then obtained by a Kramers-Kronig transformation,

$$\text{Re}\Sigma(k, \omega) = V_{\text{ex}}(k) + \frac{P}{\pi} \int \frac{\text{Im}\Sigma(k, \omega') d\omega'}{\omega - \omega'}, \quad (\text{B4})$$

where

$$V_{\text{ex}}(k) = -\frac{2}{\pi} \left[ \frac{k_F}{2} + \frac{k_F^2 - k^2}{4k} \ln \left| \frac{k + k_F}{k - k_F} \right| \right], \quad (\text{B5})$$

is the energy-independent part in  $\Sigma$ , i.e., the Hartree-Fock exchange energy. In the calculations presented in this work we have chosen the plasmon dispersion as in Ref. 20, i.e.,  $\alpha = 2/3$ , which is the same as that used in the extrinsic loss calculations in the FEFF8 code.

- 
- <sup>1</sup>J. J. Rehr, E. A. Stern, R. L. Martin, and E. R. Davidson, Phys. Rev. B **17**, 560 (1978).  
<sup>2</sup>W. Bardyszewski and L. Hedin, J. Phys. Colloq. **48**, C9 (1987).  
<sup>3</sup>L. Hedin, Physica B **158**, 344 (1989).  
<sup>4</sup>J. E. Inglesfield, Solid State Commun. **40**, 467 (1981); J. Phys. C **16**, 403 (1983).  
<sup>5</sup>W. Bardyszewski and L. Hedin, Phys. Scr. **32**, 439 (1985).  
<sup>6</sup>T. Fujikawa, J. Phys. Soc. Jpn. **62**, 2155 (1993).  
<sup>7</sup>F. Aryasetiawan, L. Hedin, and K. Karlsson, Phys. Rev. Lett. **77**, 2268 (1996).  
<sup>8</sup>L. Hedin and S. Lundqvist, Solid State Phys. **21**, 1 (1969).  
<sup>9</sup>L. Hedin, Phys. Scr. **21**, 477 (1980).  
<sup>10</sup>J. J. Rehr and R. C. Albers, Rev. Mod. Phys. **72**, 621 (2000).  
<sup>11</sup>J. J. Rehr, R. C. Albers, and S. I. Zabinsky, Phys. Rev. Lett. **69**, 3397 (1992).  
<sup>12</sup>T. Jo and G. A. Sawatzky, Phys. Rev. B **43**, 8771 (1991); G. van der Laan and B. T. Thole, J. Phys.: Condens. Matter **4**, 4181 (1992).  
<sup>13</sup>D. C. Langreth, Phys. Rev. B **1**, 471 (1970).  
<sup>14</sup>C.-O. Almbladh and L. Hedin, in *Handbook on Synchrotron Radiation*, edited by E. E. Koch (North Holland, Amsterdam, 1983), pp. 607–904.  
<sup>15</sup>P. Lloyd, J. Phys. F: Met. Phys. **1**, 728 (1971).  
<sup>16</sup>L. Hedin, J. Michiels, and J. Inglesfield, Phys. Rev. B **58**, 15 565 (1998).  
<sup>17</sup>L. Hedin, J. Phys.: Condens. Matter **11**, R489 (1999).  
<sup>18</sup>A. L. Ankudinov, B. Ravel, J. J. Rehr, and S. D. Conradson, Phys. Rev. B **58**, 7565 (1998).  
<sup>19</sup>J. R. Schrieffer, Phys. Scr. **21**, 472 (1980).  
<sup>20</sup>B. I. Lundqvist, Phys. Kondens. Mater. **6**, 193 (1967).